

# Superfluid Field response to Edge dislocation motion

Abdul N. Malmi-Kakkada,<sup>1,2,\*</sup> Oriol T. Valls,<sup>1,†</sup> and Chandan Dasgupta<sup>3,‡</sup>

<sup>1</sup>*School of Physics and Astronomy, University of Minnesota, Minneapolis, Minnesota 55455*

<sup>2</sup>*Department of Chemistry, University of Texas, Austin, Texas, 78712*

<sup>3</sup>*Centre for Condensed Matter Theory, Department of Physics,  
Indian Institute of Science, Bangalore 560012, India*

(Dated: April 7, 2017)

We study the dynamic response of a superfluid field to a moving edge dislocation line to which the field is minimally coupled. We use a dissipative Gross-Pitaevskii equation, and determine the initial conditions by solving the equilibrium version of the model. We consider the subsequent time evolution of the field for both glide and climb dislocation motion and analyze the results for a range of values of the constant speed  $V_D$  of the moving dislocation. We find that the type of motion of the dislocation line is very important in determining the time evolution of the superfluid field distribution associated with it. Climb motion of the dislocation line induces increasing asymmetry, as function of time, in the field profile, with part of the probability being, as it were, left behind. On the other hand, glide motion has no effect on the symmetry properties of the superfluid field distribution. Damping of the superfluid field due to excitations associated with the moving dislocation line occurs in both cases.

## I. INTRODUCTION

Supersolids represent an exotic state of quantum matter in which two kinds of order exist simultaneously: crystalline order associated with the breaking of translational symmetry and superfluid order associated with the breaking of the symmetry under a global rotation of the quantum mechanical phase. The possibility of occurrence of a supersolid phase in solid  $^4\text{He}$  was pointed out [1–3] many years ago. More recently, supersolid phases have been realized in experiments on ultracold atomic systems. The first experimental observations of a supersolid phase [4–6] involved the self-organization of a Bose-Einstein condensate (BEC) in which the discrete translational symmetry of a preimposed lattice structure was spontaneously broken. Recent experiments [7, 8] have demonstrated the occurrence of supersolid phases in which the continuous translational symmetry of space is spontaneously broken. One of these experiments [7] involves a BEC with spin-orbit coupling that exhibits a supersolid stripe phase with density modulation in one direction. The other experiment [8] involves a BEC dispersively coupled to two optical cavities. Many other proposals for the occurrence of supersolid phases in ultracold atomic systems exist in the literature [9–12] and it is expected that some of these proposals will be realized in experiments in the near future. Therefore, studies of various physical properties of quantum solids in the presence of superfluidity are of much current interest.

Topological defects of crystalline solids are dislocations

which form a network of lines in three dimensional systems. There exists a vast literature [13] on the properties of dislocations in conventional solids. Dislocations play a very important role in the mechanical response of crystalline solids. When a crystalline solid is subjected to an external stress, the response of the solid is determined to a large extent by the motion of dislocations induced by the stress. The properties of dislocations in supersolids is relatively less understood. The motion of a dislocation line in a supersolid is more complicated than that in a conventional crystal because of the presence of superfluidity. The motion of a dislocation line in a supersolid affects the superfluidity in its vicinity because the superfluid order parameter is coupled to the strain field of the dislocation line. This coupling also changes parameters such as the mobility associated with the motion of dislocation lines. This interplay between the motion of a dislocation line and superfluidity in its neighborhood is the subject of our study. Dislocations in the vortex lattice in a rotating BEC [14] provide another example of a cold matter system in which this interplay between crystal defects and superfluidity plays an important role.

This subject is also important for understanding the low-temperature properties of solid  $^4\text{He}$ . Interest in the old predictions [1–3] of occurrence of supersolidity in  $^4\text{He}$  was renewed when Kim and Chan [15] observed a period drop in torsional oscillator (TO) experiments with solid  $^4\text{He}$  and interpreted the observation as evidence for the occurrence of a supersolid phase in this system at sufficiently low temperatures. Evidence that structural disorder present in samples of solid  $^4\text{He}$  could play an important role became apparent early on [16–19]: results of TO experiments were found to depend strongly on sample preparation methods, and annealing the sample was found to substantially reduce the TO period drop. Subsequently, it was found [20, 21] that an elastic anomaly with a jump in the shear modulus occurs in solid  $^4\text{He}$  at a temperature close to that of the TO period drop.

\* [naseermk@utexas.edu](mailto:naseermk@utexas.edu)

† [otvalls@umn.edu](mailto:otvalls@umn.edu); Also at Minnesota Supercomputer Institute, University of Minnesota, Minneapolis, Minnesota 55455

‡ [cdgupta@iisc.ernet.in](mailto:cdgupta@iisc.ernet.in); Also at Condensed Matter Theory Unit, Jawaharlal Nehru Centre for Advanced Scientific Research, Bangalore 560064, India

It was soon realized [22, 23] that this elastic anomaly can account for the TO period change. At present, the emerging consensus [24–26] seems to be that the anomalous low-temperature properties of solid  $^4\text{He}$  can be understood entirely in terms of the stiffening of the solid, without having to invoke the occurrence of superfluidity. The elastic anomaly is attributed to the pinning of dislocation lines by  $^3\text{He}$  impurities which prevent the dislocation lines from gliding along basal planes in solid  $^4\text{He}$ . This description accounts for several experimentally observed features [27–29] in the elastic properties of solid  $^4\text{He}$  at low temperatures.

There are, however, several experimental and theoretical results that suggest that the occurrence of superfluidity in the vicinity of defects such as dislocation lines and grain boundaries in solid  $^4\text{He}$  may play an important role in the low-temperature properties of solid  $^4\text{He}$ . Experimental observations [30, 31] of mass flow through solid  $^4\text{He}$  have been attributed to flow of atoms through superfluid dislocation cores. It has been suggested [32] that mass flow through superfluid cores of edge dislocations can lead to “superclimb” that would provide an explanation of the large isochoric compressibility observed in Ref. [30]. Results of experiments [33] on the effects of dc rotation on the TO period drop also suggest the occurrence of superfluidity. There are reports [34–36] of the occurrence of an elastic anomaly in ultra-pure samples of solid  $^4\text{He}$  in which the spacing between  $^3\text{He}$  impurities is expected to be of the order of or larger than the size of the sample. The stiffening of the solid in these samples can not be attributed to the pinning of dislocation lines by  $^3\text{He}$  impurities. It has been shown recently [37] that the onset of superfluidity in and around the cores of dislocation lines can lead to an increase of the shear modulus of the solid by decreasing the mobility of the dislocation lines. Quantum Monte Carlo calculations [38–40] have shown that superfluidity can occur in the vicinity of structural defects such as dislocations and grain boundaries in solid  $^4\text{He}$ . Theoretical studies [41, 42] indicate that a generic coupling between the superfluid field and the elastic strain field associated with a dislocation line in a phenomenological Landau theory of superfluidity leads to superfluidity in the vicinity of a stationary edge dislocation line. Theoretical studies [41–44] have also shown that bulk superfluidity can occur in solid  $^4\text{He}$  from superfluidity along a network of crystal defects. It is clear from these results that studies of superfluidity near dislocation lines in solid  $^4\text{He}$  are important, even if bulk superfluidity does not occur in this system.

In this paper, we make the assumption that superfluidity occurs near a dislocation line in a quantum crystal and examine the effect of motion of the dislocation line on superfluidity in its vicinity. Previous studies [39–43] of superfluidity near a dislocation line focused on the case where it is quenched or stationary. Many physical effects, such as the “giant plasticity” of solid  $^4\text{He}$ , attributed to nearly free gliding motion of edge dislocations along the basal planes, involve moving dislocation lines. Therefore,

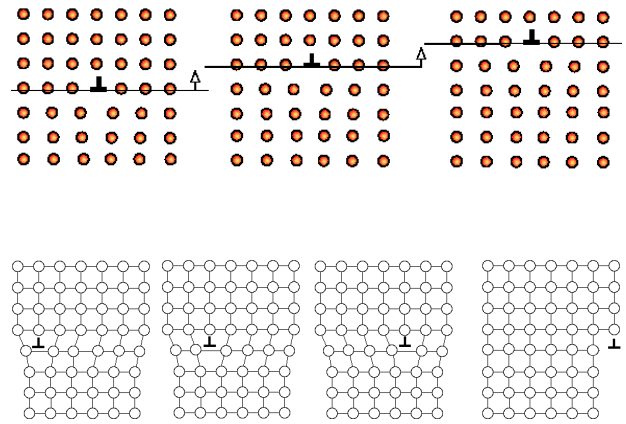


FIG. 1. Top panel: an edge dislocation is illustrated executing climb motion. The arrow indicates the direction of climb. The bottom panel illustrates the glide motion of an edge dislocation.

it is important to understand the effects of the motion of a dislocation line on the superfluidity near its core. Dislocation lines are dynamic objects that execute a variety of motions. Dislocation line segments can undergo roughening [45] and can execute two basic types of motion in response to an applied stress: climb or glide motion. These two different types of motion are illustrated in Fig. 1. When a dislocation line moves along the surface that contains both itself and the Burgers vector associated with it, the motion is called glide. Movement out of the glide surface in a direction perpendicular to the Burgers vector is referred to as climb. Glide and “superclimb” i.e. climb assisted by superfluidity in the dislocation cores in solid  $^4\text{He}$  were studied previously [46] in the context of elastic effects such as dislocation line tension and compressibility. Dislocation lines can glide freely along basal planes in solid  $^4\text{He}$  at relatively high speeds compared to other crystals. This is thought to be a quantum effect which causes the Peierls barrier to dislocation motion to be negligible [27].

Our main interest in the present study is to investigate whether the motion of a dislocation line modifies (e.g. enhances, suppresses, or distorts) the associated superfluid field. It has been suggested [47] that transverse motion of a dislocation line reduces the degree of superfluid ordering in its vicinity. A study [48] of a toy model of Ising spins residing on the links of a random network shows that motion of the links leads to a reduction in the ordering temperature of the spins. A similar effect is expected for superfluidity along a network of dislocation lines. Thus, we study here the effect of the dynamics of a dislocation line on the superfluid field at the microscopic quantum level. We have analyzed the response of the superfluid field near an edge dislocation line, assumed to be driven at constant velocity  $\vec{V}_D$ , for both climb and glide motion. Focusing on small length and time scales, we have taken into account fluctuations in both the amplitude and the phase of the superfluid order parameter.

Fluctuations in the amplitude were not included in the coarse-grained models studied earlier, because the amplitude is not a hydrodynamic variable.

A mathematical framework that has been used extensively for describing superfluidity in  $^4\text{He}$  is the Gross-Pitaevskii equation (GPE) [49, 50]. The GPE, also referred to as the nonlinear Schrödinger equation, has been quite successful in helping understand the equilibrium and dynamic behavior of low-temperature superfluids and Bose-Einstein condensates (BEC) [51]. However, the GPE does not provide a description of damping and can only be used to study dissipationless fields. As we are interested in exploring what quantum models predict for the damping of the superfluid field near a dislocation line due to its motion, a method to include dissipation in the GPE is necessary. With this purpose in mind, an approach similar to that used in Ref. [52] to study damping of superfluidity near the  $\lambda$  point is used in our study. The modification of the GPE in order to capture the effects associated with damping is referred to as the Dissipative Gross-Pitaevskii equation (DGPE) [53]. Based on the DGPE formalism and a well-studied model [41, 42] for the coupling of the superfluid field with the strain field of a dislocation line, we present in this work a study of how the excitations associated with a moving dislocation line in solid  $^4\text{He}$  affects the superfluid field near it. Both GPE and DGPE approaches have been used previously [54, 55] to study the effects of moving a line object in a superfluid. Our work is similar in spirit to these earlier studies.

We find that the motion of the dislocation line plays an important role in determining the superfluid field distribution near it. During climb motion, a part of the superfluid field associated with a stationary dislocation line is “left behind.” Climb induces more asymmetry in the distribution of the superfluid field near the dislocation line. No effect on the symmetry properties of the superfluid wavefunction is observed for glide motion. Decay of the superfluid field amplitude during climb and glide is observed, but the magnitude of the decay is very small for experimentally realistic values of the dissipation parameter.

The rest of this paper is organized as follows: Introduction of the DGPE formalism and details of the parameter values used are presented in Section II. We also provide in this Section the details of how the elastic strain field due to the dislocation is coupled to the superfluid order parameter. Results of our study of the effects of the motion of a single edge dislocation line on the superfluid field are presented in Section III. The main conclusions of our study are summarized in Section IV.

## II. METHODS

### 1. Dissipative Gross-Pitaevskii equation

We consider in this study a single long, straight edge dislocation line running along the  $z$  axis. The Burgers vector for the edge dislocation is taken to be in the  $x$ -direction. The dislocation line is assumed to be long and straight so that one can neglect edge effects and define the problem in the 2D  $x-y$  plane orthogonal to it. The standard GPE which describes the motion of a field,  $\psi$ , is of the form

$$i\hbar\frac{\partial\psi}{\partial t} = \frac{-\hbar^2}{2m}\nabla_{x,y}^2\psi + v(x,y;t)\psi + g|\psi|^2\psi, \quad (1)$$

where  $\nabla_{x,y}^2 = \frac{\partial^2}{\partial x^2} + \frac{\partial^2}{\partial y^2}$ ,  $m$  is the mass of an atom,  $v(x,y;t)$  is the potential (the time dependence arises from the dislocation motion) and  $g$  is the superfluid interaction parameter. On the right hand side, the first two terms are the kinetic and potential energy and the third, nonlinear term describes the interaction energy between superfluid atoms. This interaction is repulsive,  $g > 0$ . It is given by [9, 56]

$$g = \frac{4\pi\hbar^2 a_s N}{mL}. \quad (2)$$

Here  $a_s$  is the microscopic s-wave scattering length,  $N$  is the number of superfluid atoms and  $L$  is the size of the trap.

In the problem under study, the complex field  $\psi$  is the superfluid wavefunction, and the coupling between  $\psi$  and the dislocation strain potential is introduced via the term  $v(x,y;t)\psi$  [41]. For an edge dislocation along the  $z$ -axis the strain potential is of the form [41]

$$v(x,y) = \frac{A}{\sqrt{x^2 + y^2}} \cos\phi, \quad (3)$$

where  $\phi = \arctan(x/y)$  is an azimuthal angle defined in the  $x-y$  plane with respect to the  $y$  axis. The parameter  $A$ , a positive quantity, denotes the strength of the dislocation potential and depends on the lattice and elastic constants of the solid. For  $A > 0$ , this potential is attractive for  $y < 0$  thereby allowing for bound states. For  $y > 0$  the potential is repulsive. The potential is symmetric along the  $x$  axis (i.e. along the direction of the Burgers vector). These characteristics of the potential should be reflected on the wavefunction  $\psi$  as well.

The solution of the non-linear equation noted above is complicated due to the non-central nature of the potential [57]. The equilibrium steady state of the superfluid field at very low temperatures,  $T \rightarrow 0$ , is described by the time independent GPE

$$-\frac{\hbar^2}{2m}\nabla_{x,y}^2\psi + v(x,y)\psi + g|\psi|^2\psi = \mu\psi, \quad (4)$$

where  $\mu$  is the chemical potential. For the equilibrium solution, the wavefunction is normalized according to

$$\mathcal{N} = \int_{-\infty}^{+\infty} \int_{-\infty}^{+\infty} |\psi|^2 dx dy = 1. \quad (5)$$

The standard GPE (Eq. (1) above) contain no dissipative terms. The motion of the dislocation line is actually dissipative as a result of the various damping mechanisms within the crystal mentioned below. To account for dissipation in the GP formalism we introduce into the GPE a dimensionless damping factor  $\gamma$ , as in Ref. [53]. The resulting dissipative GPE (DGPE) is of the form

$$i\hbar \frac{\partial \psi}{\partial t} = (1 - i\gamma) \left[ -\frac{\hbar^2}{2m} \nabla_{x,y}^2 \psi + v(x, y) \psi + g|\psi|^2 \psi - \mu \psi \right], \quad (6)$$

where the positive damping factor  $\gamma$  is phenomenologically introduced in a way similar to that in Ref. [52]. The right hand side terms in the square bracket represent the change from the equilibrium state of the superfluid wavefunction due to dynamics, in our case the moving dislocation line. The damping factor  $\gamma$  is inversely proportional to a relaxation time and due to it neither the energy nor  $\mathcal{N}$  are conserved in Eq. (6). In the original study by Pitaevskii [52],  $\gamma$  was expressed in terms of the second viscosity coefficients of superfluid Helium. A similar equation with the factor  $(1 - i\gamma)$  was used in the study of soliton decay and damping of vortices [58, 59].

The dynamics of the  $\psi$  field and its damping due to elementary excitations from a moving dislocation line can now be studied within the framework of Eq. (6). By numerically solving the two-dimensional (2D) time dependent DGPE with a moving dislocation line (either climb or glide motion), the response of the superfluid order parameter  $\psi$  can now be evaluated. We consider the scenario where the dislocation line executes glide or climb at a constant velocity  $\vec{V}_D$  due to external forces.

Prior to presenting the details of the numerical calculation, we need to give an overview of the units used. It is convenient to rescale the length and time in terms of natural units. We choose for our unit of length the elastic correlation length  $\xi_{el}$  defined by equating the kinetic energy of the superfluid to the potential energy due to the dislocation line,  $\hbar^2/2m\xi_{el}^2 = A/\xi_{el}$ . Similarly, we rescale time by the characteristic frequency  $\omega_{el} \equiv \hbar/2m\xi_{el}^2$ . Rescaling the wave function, the cartesian co-ordinates  $x, y$  as defined above, and the time via the definitions  $\bar{t} \equiv \omega_{el} t$ ,  $\bar{\psi} \equiv \psi \xi_{el}$ ,  $\bar{x} \equiv x/\xi_{el}$  (similarly for  $\bar{y}$ ),  $\bar{v} \equiv v/\hbar\omega_{el}$ ,  $\bar{g}|\bar{\psi}|^2 \equiv g|\psi|^2/\hbar\omega_{el}$  and  $\bar{\mu} \equiv \mu/\hbar\omega_{el}$  one obtains

$$i \frac{\partial \bar{\psi}}{\partial \bar{t}} = (1 - i\gamma) \left[ -\bar{\nabla}_{\bar{x}, \bar{y}}^2 \bar{\psi} + \bar{v}(\bar{x}, \bar{y}; \bar{t}) + \bar{g}|\bar{\psi}|^2 \bar{\psi} - \bar{\mu} \bar{\psi} \right]. \quad (7)$$

The coefficient of the non-linear term is  $\bar{g} \equiv 2mg/\hbar^2$  and the strength of the dislocation potential,  $A$ , is rescaled such that  $\bar{A} = A/\hbar\omega_{el}\xi_{el} = 1$  consistent with the definition of  $\xi_{el}$  and  $\omega_{el}$ .

## 2. Numerical parameters and initial condition

We now discuss the numerical values of the parameters used in solving Eq. (7). The time dependent strain potential  $v(x, y; t)$  in the DGPE depends upon whether the dislocation line is climbing or gliding. For climb motion, along the positive  $y$ -axis (perpendicular to the Burgers vector), the dislocation potential depends on the speed  $V_D$  via

$$v(x, y; t) = \frac{A}{\sqrt{x^2 + (y - V_D t)^2}} \cos \phi. \quad (8)$$

When the dislocation is caused to move in the direction of the Burgers vector along the  $x$  axis, i.e. with the corresponding potential being

$$v(x, y; t) = \frac{A}{\sqrt{(x - V_D t)^2 + y^2}} \cos \phi \quad (9)$$

it executes glide motion. Climb and glide motion of the dislocation line are considered separately in this study.

The magnitude of the climb and glide velocity in classical crystals is expected to be small especially at low temperatures. In a quantum crystal such as solid  $^4\text{He}$ , however, the possibility of superclimb and glide assisted by superfluidity [46] requires one to include larger values of the velocity. Glide velocities up to 0.01 m/s are considered in an experimental study [28] of dislocation velocities in solid  $^4\text{He}$ . We take  $V_D$  near its upper range to be better able to numerically observe its effects. To estimate the order of magnitude of  $\xi_{el}$ , the strength of the dislocation potential  $A$  (see Eq. (3)) a characteristic quantity with dimensions of energy $\times$ length, is needed. The magnitude of the parameter  $A$  depends on the energy per unit length of an edge dislocation line,  $E_{el} = Gb^2$ , where  $G$  is the shear modulus of the material and  $b$  the magnitude of the Burgers vector [13]. For  $A = E_{el}b\xi_{el}$  and using the definition of  $\xi_{el} = \hbar^2/2mA$ , for  $G \sim 60$  bar and  $b \sim 10^{-10}$  m appropriate to solid  $^4\text{He}$  [29], one obtains  $\xi_{el} \sim 10^{-9}$  m. This turns out to be roughly of the same order as the healing length [60]  $\xi_{SF}$ . Using the definition of  $\omega_{el} \equiv \hbar/2m\xi_{el}^2$ , we obtain  $\sim 10^{10}$  Hz. Hence,  $\xi_{el}\omega_{el} \sim 10$  m/s. The magnitudes of the quantities  $\xi_{el}$  and  $\omega_{el}$  set the scale for length and time dimensions in the simulation, respectively. The natural units for  $V_D$  are  $\xi_{el}\omega_{el}$ . Dimensionless values for the magnitude of  $V_D$  ranging from  $5 \times 10^{-4}$  to  $1.5 \times 10^{-3}$  (i.e. between 0.005 m/s and 0.015 m/s, consistent with the experimental [28] range) are used for both climb and glide motion in our computations. These are much smaller than the speed of sound, which is on the order of  $10^2$  m/s.

The strength of the interaction coefficient can be rewritten as  $\bar{g} \equiv 8\pi a_s \rho_{2D} \xi_{el}$  given  $\bar{g} \equiv 2mg/\hbar^2$  and Eq. (2). Here, the number density of superfluid atoms in 2D is  $\rho_{2D} = N/\xi_{el}^2$ . The atomic number density of solid  $^4\text{He}$  is  $\rho_{3D} = 10^{28}/\text{m}^3$  [61]. For the spacing between atomic planes at  $\sim 3 \times 10^{-10}$  m [62], the number density in 2D (i.e. per atomic plane) is  $3 \times 10^{18}/\text{m}^2$ . The scattering



length,  $a_s$ , for  $^4\text{He}$  atoms is  $\simeq 10^{-10}m$  [60]. The strength of the nonlinear interaction parameter thus obtained is  $\bar{g} \sim 7.5$ . Since we focus on the superfluid condensate density near a dislocation line, the above value for  $\rho_{2D}$  would greatly overestimate the condensate density. Assuming that a small percentage of atoms of order 1% condense into the superfluid state [40, 63] near the dislocations, a smaller value for  $\bar{g} \sim 0.075$  is obtained. This is the value of  $\bar{g}$  we use throughout this study.

In order to solve Eq. (7), the value of the chemical potential  $\bar{\mu}$  is needed. To obtain  $\bar{\mu}$ , the steady state GPE (see Eq. (4)) is numerically solved using a relaxation method under the condition that  $\psi$  satisfies Eq. (5). The accuracy of this method was tested using the two dimensional Coulomb potential, the solutions of which are well known [57]. Length and time units were properly rescaled in terms of the units in Ref. [57] for these purposes. Using this procedure, the value  $\bar{\mu} = -0.13$  was obtained for our system, consistent with other calculations [57] of the same parameter for a two dimensional Schrödinger equation with a non-moving dislocation line potential.

The value of the dimensionless damping parameter  $\gamma$  is also needed in order to solve the DGPE. In Ref. [53], the magnitude of  $\gamma$  was found to depend on the rate at which thermal particles above the Bose-Einstein condensate band enter the condensate. This rate, compared to the relevant trap frequency, sets the order of magnitude of  $\gamma$ . Using a similar approach, comparing the energy dissipated by a moving dislocation line to the energy scale  $\hbar\omega_{el}$ , an estimate for  $\gamma$  appropriate for the problem under consideration can be obtained. The energy dissipated during dislocation motion is roughly  $F_D L_D b$  where  $F_D$  is the force per unit length applied on a dislocation,  $L_D$  is the typical length of a dislocation line and  $b$  the magnitude of Burgers vector. The orders of magnitude of these quantities for a dislocation line in solid  $^4\text{He}$  were obtained from Ref. [29] where  $F_D \sim 10^{-12} - 10^{-13} \text{N/m}$  and  $L_D \sim 10^{-4}m$ . The value of the parameter  $\gamma \sim F_D L_D b / \hbar\omega_{el}$  thus obtained is  $\sim 10^{-3}$ . In our calculations, we set  $\gamma = 10^{-3}$ , unless stated otherwise.

Next, we need to discuss the initial conditions chosen and the numerical method used in our computations. The equilibrium solution obtained from the time independent GPE (Eq. (4)) is set as the initial condition for  $\psi$  in solving the time dependent Eq. (7). At,  $\bar{t} = 0$ , the dislocation line is stationary and the superfluid distribution around it corresponds to the equilibrium case. As the dislocation line starts to move, the superfluid field  $\psi$  near it reacts. The response of the superfluid field is studied for both glide and climb motion separately. Eq. (7) is solved using a split-step Crank-Nicolson method as presented in Ref. [64]. For the simulation, a  $1200 \times 1200$  square grid system with the size of each grid being  $0.05 \xi_{el}$  is used. We use fixed boundary conditions with  $\psi \equiv 0$  at the boundaries of the computational grid. A time step of  $\delta\bar{t} = 0.01$  turns out to be adequate. A small cutoff

of 0.005 for  $\bar{x}$  and  $\bar{y}$  is used in order to avoid the singularity associated with the dislocation potential at the origin. To avoid the possibility of an abrupt reaction of the superfluid field when  $\vec{V}_D$  is switched on suddenly, we turn on the velocity of the dislocation line gradually over a time  $\bar{t}_0$ , short compared with the maximum simulation time, starting at zero and ending at the desired value of  $\vec{V}_D$ . In the course of this initialization, the nonlinearity parameter  $\bar{A}$  is slowly incremented to its value. The value  $\bar{t}_0 \sim 100$  is used. The results have been verified to be independent of the small cutoff and insensitive to the precise value of  $\bar{t}_0$ .

The scenarios considered here can easily be related to experimental situations. Applying a stress on  $^4\text{He}$  crystal causes the dislocation line to move. The contribution of factors such as thermal phonons or other impurities present in the crystal to damping of dislocation motion was discussed in Ref. [29]. The parameter  $\gamma$  takes into account the effect on the superfluid field due to such excitations, as they may be induced by the dissipative motion of a dislocation line. In the results presented below, we investigate how climb and glide motion affects the superfluid field in its vicinity.

### III. RESULTS

In this Section, we present the results of our DGPE simulation coupling a moving edge dislocation line to superfluidity. We analyze the effect of the motion of a dislocation line on a superfluid field assumed to be associated with its core. The first part of this section deals with climb and the latter part with glide motion of the dislocation line. As explained above, all lengths will be given in units of  $\xi_{el}$ , time in units of  $\omega_{el}$  and velocity in terms of  $\xi_{el}\omega_{el}$ .

To obtain the initial condition, the time independent GPE (Eq. (4)) is solved to get the equilibrium solution for the superfluid field  $|\bar{\psi}|$  near an edge dislocation line, using the stationary potential as given in Eq. (3). Results are shown in Fig. 2. The absolute value of the dimensionless equilibrium wave function,  $|\bar{\psi}|$ , near an edge dislocation line, is plotted there. The results are given in the form of 3D plots of the superfluid distribution. Two different viewing orientations are shown in that figure, specifically, views along the  $\bar{y}$  axis and  $\bar{x}$  axis are presented in the top and bottom panels respectively. It can be seen that a bound state of the superfluid field forms in the attractive part of the dislocation potential (in the  $\bar{y} < 0$  region). The dislocation potential is symmetric along the  $\bar{x}$  axis with respect to the origin, and asymmetric along the  $\bar{y}$  axis. The symmetry characteristics of the potential can be seen reflected in  $|\bar{\psi}|$ : an asymmetric accumulation of the superfluid field in the region  $\bar{y} < 0$  can be observed.

To study the effect of a climbing dislocation on the superfluid field, we solve the DGPE (Eq. (7)) with the dislocation potential now taking the form as in Eq. (8) and the initial condition presented above. Given that a

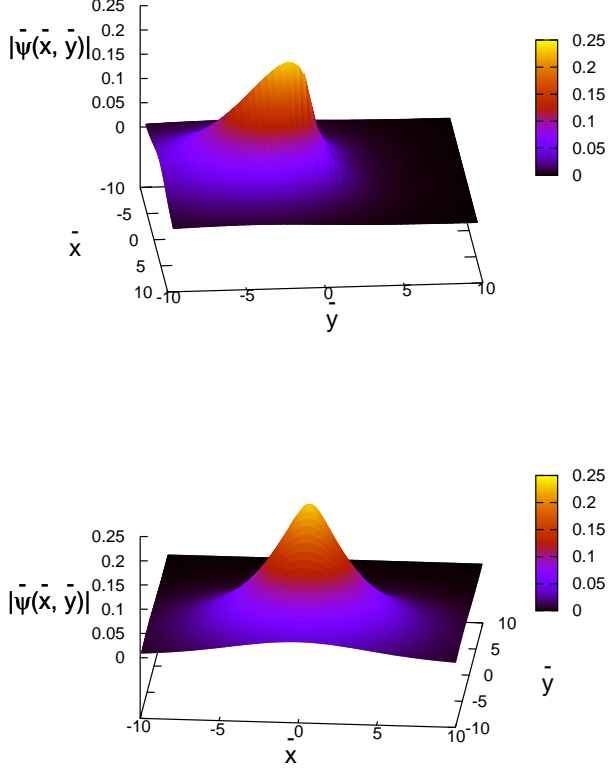


FIG. 2. The absolute value of the equilibrium  $|\bar{\psi}(\bar{x}, \bar{y})|$  of the superfluid field. A broad maximum is seen in the attractive region of the dislocation strain potential. The two plots correspond to different visual orientations (see text). Results were obtained by solving Eq. (4).

stationary dislocation line enhances superfluidity[41] in its vicinity, one naively expects that the motion of the dislocation line could ‘smear’ the superfluid field over a larger region. This could then perhaps suppress the effectiveness of the dislocation line in enhancing superfluidity, as compared to the stationary case. In the results presented in Fig. 3, the dislocation line is assumed to move along the positive  $y$  direction (climb) at two different speeds namely  $V_D = 5 \times 10^{-4}$  and  $1.5 \times 10^{-3}$  in our dimensionless units. The value  $7.5 \times 10^{-4}$  was also studied, yielding intermediate results. The response of the superfluid field due to this dislocation line motion is illustrated in Fig. 3 through a plot of  $|\bar{\psi}(\bar{x} = 0, \bar{y}; \bar{t})|$  at different times. At any time  $\bar{t}$ , the dislocation line is displaced in the positive  $y$  direction by a distance  $V_D \bar{t}$ . The top panel of Fig. 3 shows a plot of  $|\bar{\psi}(\bar{x} = 0, \bar{y}; \bar{t})|$  at  $\bar{t} = 0, 6000$ , and  $14000$  for  $V_D = 5 \times 10^{-4}$ . The bottom panel shows the same quantity for  $V_D = 1.5 \times 10^{-3}$  at three different values of  $\bar{t}$ ,  $\bar{t} = 0, 4000$ , and  $6000$ . For  $\bar{t} = 6000$  and  $V_D = 1.5 \times 10^{-3}$ , (bottom panel) the dislocation line has moved a distance of magnitude  $\sim 9$ , while the corresponding maximum distance in the top panel is  $\sim 7$ . The

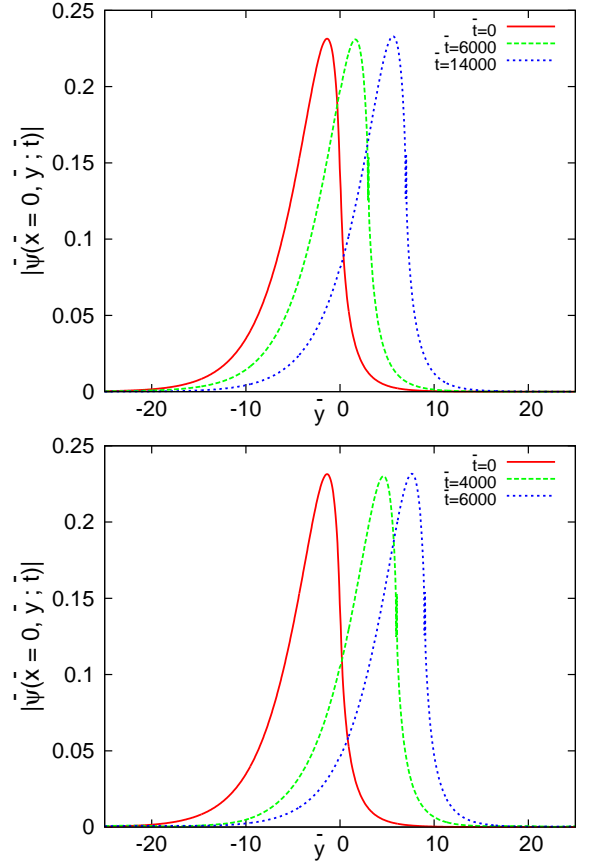


FIG. 3. Plot of the absolute value of the wavefunction,  $|\bar{\psi}(\bar{x} = 0, \bar{y}; \bar{t})|$  at different times for a climbing edge dislocation line. The top panel corresponds to  $V_D = 5 \times 10^{-4}$  and the bottom panel to  $V_D = 1.5 \times 10^{-3}$ . The times are indicated in the legend.

shift in the superfluid distribution as a result of dislocation motion at other values of  $\bar{t}$  and  $V_D$  can be clearly observed. The plot of  $|\bar{\psi}(\bar{x} = 0, \bar{y}; \bar{t})|$  has a maximum at a location  $\bar{y} \equiv \bar{y}_{max}$ . At  $\bar{t} = 0$ ,  $\bar{y}_{max}$  is at  $-1.3$ .

As the dislocation line executes climb motion, it appears from the figures that the superfluid distribution becomes more asymmetric in the  $y$  direction. This increase in asymmetry, with a longer tail towards the smaller  $y$  region (between negative values of  $\bar{y}$  till  $\bar{y}_{max}$ ), might be thought of as if some of the superfluid amplitude were ‘left behind’ i.e. as the dislocation line moves it ‘smears’ the superfluid field over a wider region. In order to make this more evident, and to quantify it, we define an asymmetry parameter  $B$ . The  $B$  parameter is defined in terms of the integrated norm of superfluid field in the region  $\bar{y} < \bar{y}_{max}$  vs in the region  $\bar{y} > \bar{y}_{max}$  over the 2D  $x - y$  plane, in this way:

$$B = \frac{\int_{-\infty}^{+\infty} \int_{-\infty}^{\bar{y}_{max}} |\bar{\psi}|^2 d\bar{x} d\bar{y} - \int_{-\infty}^{+\infty} \int_{\bar{y}_{max}}^{+\infty} |\bar{\psi}|^2 d\bar{x} d\bar{y}}{\int_{-\infty}^{+\infty} \int_{-\infty}^{\bar{y}_{max}} |\bar{\psi}|^2 d\bar{x} d\bar{y} + \int_{-\infty}^{+\infty} \int_{\bar{y}_{max}}^{+\infty} |\bar{\psi}|^2 d\bar{x} d\bar{y}}. \quad (10)$$

The procedure implied by this definition is illustrated in

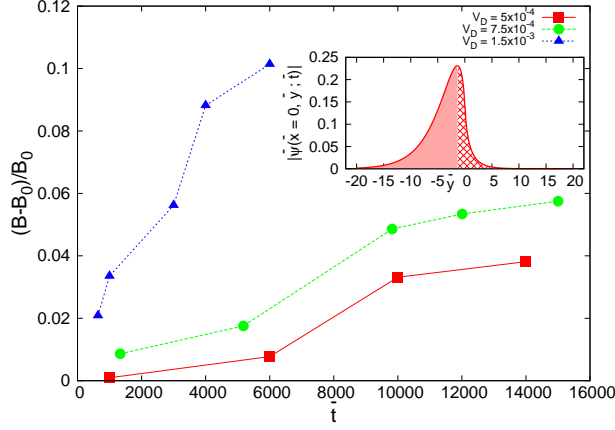


FIG. 4. The asymmetry parameter  $(B - B_0)/B_0$  (see text) during climb motion is shown as a function of time  $\bar{t}$  in the main plot for three different values of  $V_D$  as indicated in the legend. The inset illustrates the procedure employed to extract  $B$  as defined in Eq. (10). The value for  $B_0 = 0.538$ .

the inset of Fig. 4: the contribution to the first term in the numerator of  $B$  in Eq. (10) is shaded in solid color along the plane defined by  $\bar{x} = 0$ . Similarly, the contribution to the second term in the numerator is marked by the hatched region. Due to the motion of the dislocation line in the positive  $y$  direction, if the superfluid field is ‘left behind’, the distribution of  $|\bar{\psi}|$  in the region  $\bar{y} < \bar{y}_{max}$  will increase while decreasing in the region  $\bar{y} > \bar{y}_{max}$ . The time dependent parameter  $B$  can therefore be used to measure the asymmetry in the distribution of the superfluid field due to dislocation movement. The equilibrium solution shown in Fig. 3 i.e.  $|\bar{\psi}(\bar{x} = 0, \bar{y}; \bar{t} = 0)|$  is asymmetric along the  $y$  direction and has a non zero value of the asymmetry parameter,  $B(\bar{t} = 0) = B_0$ . To study the change in asymmetry due to climb motion, we look at  $(B - B_0)/B_0$  as a function of  $\bar{t}$ . A plot of  $(B - B_0)/B_0$  vs  $\bar{t}$  is presented in the main part of Fig. 4. Results for the three different values of  $V_D$  mentioned above are given. The asymmetry of the superfluid field near the dislocation line and along the direction of motion increases due to climb. It is also seen that the rate of increment of parameter  $B$  slows as the dislocation line evolves for longer times. For higher climb velocities, more of the superfluid field tends to be ‘left behind’: faster moving dislocations leave behind more of the superfluid field. Examination of the wavefunction at  $\bar{y} = \bar{y}_{max}$  i.e.  $|\bar{\psi}(\bar{x}, \bar{y} = \bar{y}_{max}; \bar{t})|$  shows that climb has no effect on the wavefunction shape in the  $x$  direction. No change in superfluid field distribution is observed perpendicular to the direction of climb motion.

Next, we consider glide motion of the dislocation line and the response of the superfluid field to it. We solve the DGPE with the dislocation potential given in Eq. (9) for glide along the positive  $x$  direction. The top panel of Fig. 5 shows  $|\bar{\psi}(\bar{x}, \bar{y} = \bar{y}_{max}; \bar{t})|$  at  $\bar{t} = 0, 2196$  and  $6590$  for  $V_D = 5 \times 10^{-4}$ . The superfluid field is carried along with the dislocation line. The maximum of  $|\bar{\psi}|$  at

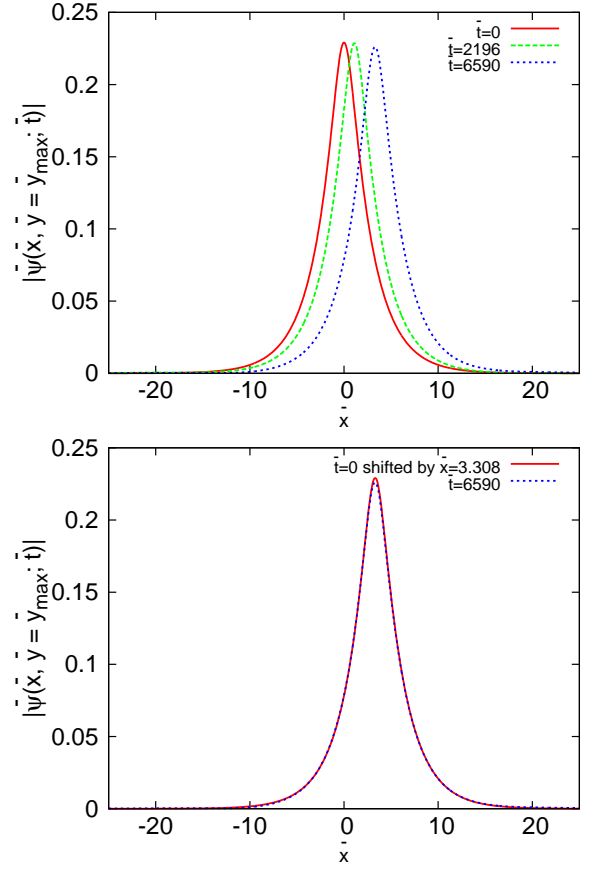


FIG. 5. In the top panel, the absolute value of the wave function  $|\bar{\psi}(\bar{x}, \bar{y} = \bar{y}_{max}; \bar{t})|$  is shown for  $\bar{t} = 0, 2196$  and  $6590$  during glide.  $V_D = 5 \times 10^{-4}$  is used. In the bottom panel, the equilibrium  $|\bar{\psi}(\bar{x} = \bar{x}_{max}, \bar{y}; \bar{t} = 0)|$  is offset by  $\bar{x} = 3.308$  along the positive  $x$  direction in order to compare it to  $|\bar{\psi}(\bar{x}, \bar{y} = \bar{y}_{max}; \bar{t} = 6590)|$ .

$\bar{y} = \bar{y}_{max}$  shifts from  $\bar{x} = 0$  to a value corresponding to  $V_D \bar{t}$  referred to as  $\bar{x}_{max}$ . After  $\bar{t} = 6590$ , the maximum of  $|\bar{\psi}|$  along  $\bar{y}_{max}$  is expected to shift by  $V_D \bar{t} = 3.3$ , matching the simulation results. We look again for evidence of asymmetry developing in the superfluid distribution due to glide motion. Glide evolution of  $|\bar{\psi}|$  along the  $x$  direction does not alter its symmetry or its shape at all, as is evident from the bottom panel of Fig. 5. The  $\bar{y} = \bar{y}_{max}$  cross section of the equilibrium solution ( $\bar{t} = 0$ ) is shifted by  $\bar{x} = 3.308$  in order to compare it to the time evolved wave function  $|\bar{\psi}(\bar{x}, \bar{y} = \bar{y}_{max}; \bar{t} = 6590)|$ . No change in the symmetry characteristics for  $|\bar{\psi}|$  along  $\bar{y} = \bar{y}_{max}$  is observed, confirming that glide motion does not leave behind the superfluid field along the direction of motion. Similarly, a plot of  $|\bar{\psi}|$  for glide motion along the perpendicular direction at  $\bar{x} = \bar{x}_{max}$ , is presented in Fig. 6. We compare there  $|\bar{\psi}(\bar{x} = \bar{x}_{max}, \bar{y}; \bar{t})|$  at  $\bar{t} = 0$  and  $6590$ . No change in the shape is observed.

We have also studied the time dependence of the total normalization of the wavefunction ( $\mathcal{N}$  see Eq. (5)). As noted earlier, the damping factor  $\gamma$  in the DGPE implies

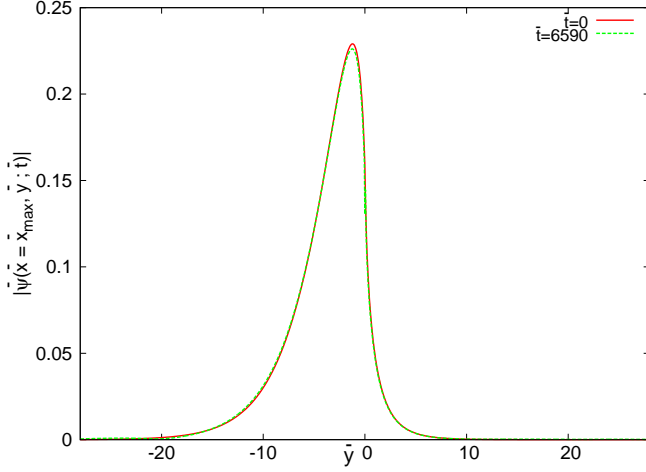


FIG. 6. Plot of  $|\bar{\psi}(\bar{x} = \bar{x}_{max}, \bar{y}; \bar{t})|$  at  $\bar{t} = 0$  and  $\bar{t} = 6590$  during glide for  $V_D = 5 \times 10^{-4}$ . No change in the shape  $|\bar{\psi}|$  along  $\bar{x} = \bar{x}_{max}$  is observed.

that  $\mathcal{N}$  is not conserved.  $\mathcal{N}$  for the superfluid field is observed to decrease for both climb and glide motion. Plots of  $\mathcal{N}$  vs  $\bar{t}$  for climb and glide motion at three different values of  $\gamma$  are presented in the top panel of Fig. 7. The decay in  $\mathcal{N}$  as a result of glide motion at  $V_D = 5 \times 10^{-4}$  for  $\gamma = 10^{-3}$  is too small to be seen and unimportant. An artificially larger value of  $\gamma = 10^{-1}$  is used to amplify any possible decay effect. This results in a  $\sim 5\%$  decay in  $\mathcal{N}$  over a time interval of 800 for glide. Climb motion also results in the damping of superfluidity near an edge dislocation line. At  $\gamma = 10^{-3}$ , again, the decay in  $\mathcal{N}$  is minute. Using a larger value of  $\gamma = 10^{-1}$  the decay effect is much more visible. Approximately a 30% decay in  $\mathcal{N}$  can now be observed over a time interval of 800. Overall, in comparing climb and glide motion, the decay in  $\mathcal{N}$  is much more pronounced due to climb.

The physical origin of the decay in  $\mathcal{N}$  can be roughly understood from the following arguments. Rewriting the DGPE in Eq. (6) as

$$i\hbar \frac{\partial \psi}{\partial t} = (1 - i\gamma)[H - \mu]\psi, \quad (11)$$

where  $H = -\frac{\hbar^2}{2m} \nabla_{x,y}^2 + v(x, y) + g|\psi|^2$  it can be seen from Eq. (4) that  $H\psi = \tilde{\mu}(t)\psi$ . By rescaling  $t$  in the equation above to  $t' = (1 - i\gamma)t$  a solution of the form  $\psi = \psi_0 e^{-i\Delta\tilde{\mu}(t)t'}$  is obtained where  $\Delta\tilde{\mu}(t) \equiv \tilde{\mu}(t) - \mu$  is the change in the effective chemical potential. This implies that

$$\psi = \psi_0 e^{-(i/\hbar)(\tilde{\mu}(t) - \mu)t} e^{-(\gamma/\hbar)(\tilde{\mu}(t) - \mu)t}, \quad (12)$$

where the damping contribution to  $\psi$  can be seen to depend on  $\gamma$  and  $\tilde{\mu}(t) - \mu$ . At  $\gamma = 0$  no decay in  $\mathcal{N}$  is observed consistent with what is expected from Eq. 12. The quantity  $\tilde{\mu}(t) - \mu$  in dimensionless units turns out to be roughly of order  $V_D$ . The faster the motion of the dislocation line, the larger the change  $\Delta\mu(t)$ .

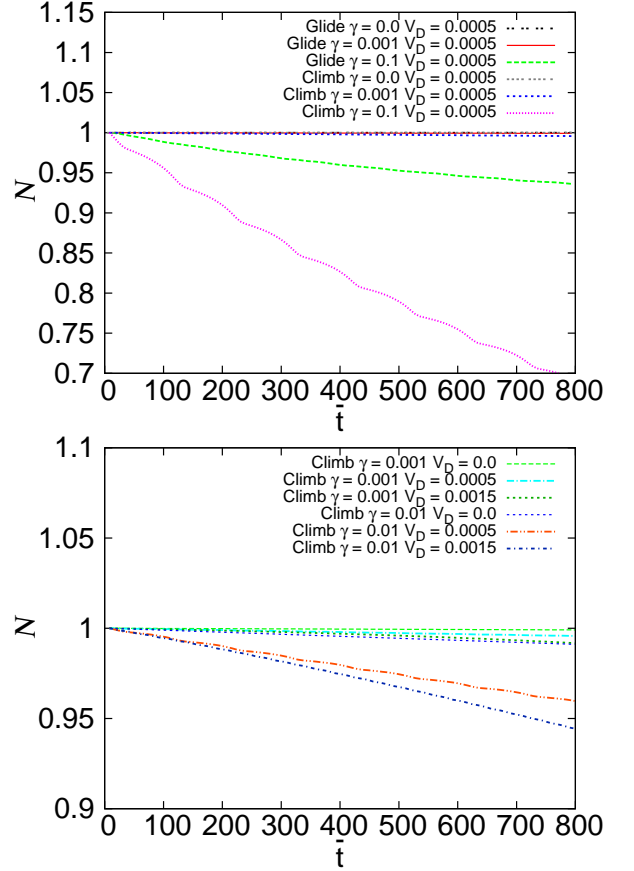


FIG. 7. Plots of the total normalization  $\mathcal{N}$  vs  $\bar{t}$ . In the top panel, three different values of  $\gamma = 0$ ,  $10^{-3}$  and  $10^{-1}$  are used for both climb and glide motion at a fixed velocity of  $V_D = 5 \times 10^{-4}$ . In the bottom panel the change in  $\mathcal{N}$  at varying velocities  $V_D = 0$ ,  $5 \times 10^{-4}$ ,  $1.5 \times 10^{-3}$  for climb at two different values of  $\gamma = 10^{-3}$ ,  $10^{-2}$  is shown.

In the bottom panel of Fig. 7 we study the effect of climb velocity (we have already seen that glide is less effective) on the damping of the superfluid field near the dislocation line at  $\gamma = 10^{-3}$  and an intermediate value  $\gamma = 10^{-2}$ . At  $V_D = 0$  and  $\gamma = 10^{-3}$ , the decay in  $\mathcal{N}$  is too small to be seen. For larger values of  $V_D$ , the decay in the superfluid field is larger. This can be understood by considering that motion of the dislocation line introduces excitations into the system thereby raising the  $\tilde{\mu}(t)$ . The excitations are responsible for the decay in the superfluid field amplitude. We see then that for realistic values of  $\gamma$  the effect on the overall normalization is quite small for either climb or glide motion.

#### IV. CONCLUSION

In this paper we have studied, at the microscopic level, the dynamic response of a superfluid field associated with an edge dislocation line which is moving at a constant speed  $V_D$ . Both types of dislocation motion (climb and



glide) are analyzed, for several values of  $V_D$ . We use the dissipative Gross-Pitaevskii equation: damping of the superfluid field due to dislocation motion is taken into account via a damping factor  $\gamma$ , as seen in Eq. (7). We use a split-step Crank-Nicolson method [64] to solve the DGPE. The results provide insight into how the dislocation motion influences the evolution of the superfluid distribution and its damping.

We determine our initial conditions by solving the equilibrium GPE for the superfluid field minimally coupled to a stationary dislocation line. This solution shows the enhancement of superfluidity near the dislocation line - the dislocation strain potential acts as a trap for the superfluid field. Hence the equilibrium wave function  $|\psi(\bar{x}, \bar{y}; \bar{t} = 0)|$  reflects the symmetry characteristics of the strain potential: it is symmetric in  $x$  (the direction of the Burgers vector) at fixed  $y$ , e.g.  $\bar{y} = \bar{y}_{max}$  and asymmetric in  $y$  at fixed  $x$ , e.g.  $\bar{x} = 0$ . We then solve for the time dependent field when the dislocation moves. We find that the superfluid field response to climb shows evidence of superfluidity being ‘left behind’ the moving dislocation: the superfluid distribution becomes increasingly asymmetric along the direction of climb. We introduce (see Eq. (10) and Fig. 4) an asymmetry parameter  $B$  to quantify how the superfluid field is being ‘left behind.’ The parameter  $B$  increases as a function of time: it rises quickly at shorter times and flattens as the dislocation line evolves over a longer time. This is consistent with earlier proposals [47], that fluctuations associated with a dislocation line can be expected to suppress the associated superfluid field, possibly by smearing it over a wider region. The magnitude of the asymmetry parameter  $B$  increases as the dislocation line moves faster. At higher speeds, the superfluid field is smeared or left behind over a larger area. Therefore, a sudden change in the position of the dislocation line makes it more difficult for the superfluid field to be trapped in the dislocation potential.

For glide motion, we have also analyzed the symmetry characteristics of the wave function at fixed  $\bar{x} = \bar{x}_{max}$  and at fixed  $\bar{y} = \bar{y}_{max}$ . In this case, as opposed to what occurs for climb motion, no change in the superfluid distribution symmetry characteristics are noted along the glide direction. We therefore identify a clear difference in the superfluid response to climb as compared to glide motion: while climb tends to leave behind the initially trapped superfluid field, glide movement is quite effective in ‘carrying along’ the superfluid field.

Both dislocation climb and glide lead to a small decay in the superfluid wavefunction normalization ( $\mathcal{N}$ ) for the physical value of  $\gamma = 10^{-3}$  considered in this study. Using a larger value of  $\gamma = 10^{-1}$ , a much larger decay effect can be observed. As the parameter  $\gamma$  takes into account the energy dissipated by the dislocation motion, larger values of  $\gamma$  must indeed, as shown, lead to more damping of the associated superfluid field. By studying the fluctuations in the amplitude of the superfluid field, a non-hydrodynamic variable, within the DGPE formalism, we observe similar trends in the asymmetric distribution of the superfluid field (as quantified by the parameter  $B$ ) and the decay in superfluid wavefunction normalization. Faster motion of the dislocation line leads to both larger decay of the superfluid field and increased asymmetry in its spatial distribution. The coupling between the damping parameter  $\gamma$  and  $V_D$  is clearly elucidated.

In summary, we have studied the effects of dislocation motion on an associated superfluid field. During glide, no change in the superfluid field asymmetry characteristics is observed. However, climb motion leads to the superfluid field being asymmetrically smeared near the dislocation line. The asymmetry induced in the superfluid distribution due to climb is the most prominent physical effect observed in this study. The implication of dislocation motion in terms of the decay of the superfluid field is also discussed.

- 
- [1] A. F. Andreev and I. M. Lifshitz, Sov. Phys. JETP **29**, 1107 (1969).
  - [2] A. J. Leggett, Phys. Rev. Lett. **25**, 1543 (1970).
  - [3] G. V. Chester, Phys. Rev. A **2**, 256 (1970).
  - [4] K. Baumann, C. Guerlin, F. Brennecke, and T. Esslinger, Nature **464**, 1301 (2010).
  - [5] R. Mottl, F. Brennecke, K. Baumann, R. Landig, T. Donner, and T. Esslinger, Science **336**, 1570 (2012).
  - [6] R. Landig, L. Hruby, N. Dogra, M. Landini, R. Mottl, T. Donner and T. Esslinger, Nature **532**, 476 (2016).
  - [7] J. Li, J. Lee, W. Huang, S. Burchesky, B. Shteynys, F.C. Top, A.O. Jamison and W. Ketterle, Nature **543**, 91 (2017).
  - [8] J. Leonard, A. Morales, P. Zupancic, T. Esslinger, and T. Donner, Nature **543** 87 (2017).
  - [9] I. Bloch, J. Dalibard and W. Zwerger, Rev. Mod. Phys. **80**, 885 (2008).
  - [10] F. Cinti, P. Jain, M. Boninsegni, A. Micheli, P. Zoller, and G. Pupillo, Phys. Rev. Lett. **105**, 135301 (2010).
  - [11] N. Henkel, R. Nath, and T. Pohl, Phys. Rev. Lett. **104**, 195302 (2010).
  - [12] G. Pupillo, A. Micheli, M. Boninsegni, I. Lesanovsky, and P. Zoller, Phys. Rev. Lett. **104**, 223002 (2010).
  - [13] D. Hull and D. Bacon, *Introduction to Dislocations* (Butterworth-Heinemann, Oxford, 2001).
  - [14] A. Rakonjac, A. L. Marchant, T. P. Billam, J. L. Helm, M. M. H. Yu, S. A. Gardiner, and S. L. Cornish, Phys. Rev. A **93**, 013607 (2016).
  - [15] E. Kim and M. H. W. Chan, Nature **427**, 225 (2004).
  - [16] A.S.C. Rittner, J.D. Reppey, Phys. Rev. Lett. **98**, 175302 (2007).
  - [17] A.S.C. Rittner, PhD Thesis, Cornell University, (2008).
  - [18] A. C. Clark, J. T. West, and M. H. W. Chan, Phys. Rev. Lett. **99**, 135302 (2007).
  - [19] S. Balibar and F. Caupin, J. Phys. Condens. Matter **20**, 173201 (2008).
  - [20] J. Day and J. Beamish, Nature (London) **450**, 853 (2007).

- [21] J. Day, O. Syshchenko, J. Beamish. Phys. Rev. Lett. **104**, 075302 (2010).
- [22] I. Iwasa. Phys. Rev. B **81**, 104527 (2010).
- [23] H. Maris Phys. Rev. B **86**, 020502 (2012).
- [24] J. D. Reppy, Phys. Rev. Lett. **104**, 255301 (2010).
- [25] D. Kim and M. Chan, Phys. Rev. Lett. **109**, 155301 (2012).
- [26] D.Y. Kim and M.H.W. Chan. Phys. Rev. B **90**, (2014).
- [27] A. Haziot, A.D. Fefferman, F. Souris, J.R. Beamish and S. Balibar. Phys. Rev. Lett. **110**, 035301 (2013).
- [28] A. Haziot, A.D. Fefferman, F. Souris, J.R. Beamish and S. Balibar. Phys. Rev. B **88**, 014106 (2013).
- [29] A.D. Fefferman, F. Souris, A. Haziot, J.R. Beamish and S. Balibar. Phys. Rev. B **89**, 014105 (2014).
- [30] M. W. Ray and R. B. Hallock, Phys. Rev. Lett., **100**, 235301 (2008); *ibid.* **105**, 1453018, (2010).
- [31] M. W. Ray and R. B. Hallock, J. Low Temp. Phys. **158**, 560 (2010); *ibid.* **162**, 421 (2011).
- [32] S. G. Söyler *et al.*, Phys. Rev. Lett. **103**, 175301 (2009).
- [33] H. Choi *et al.*, Science **330**, 1512 (2010); H. Choi *et al.*, Phys. Rev. Lett. **108**, 105302 (2012).
- [34] F. Souris, A.D. Fefferman, A. Haziot, N. Garroum, J.R. Beamish and S. Balibar, J. LowTemp. Phys. **178**, 149-161 (2015).
- [35] X. Rojas, C. Pantalei, H.J. Maris and S. Balibar, J. Low Temp. Phys. **158**, 478-484 (2010).
- [36] X. Rojas, A. Haziot, V. Bapst, S. Balibar and H.J. Maris, Phys. Rev. Lett. **105**, 145302 (2010).
- [37] A.N. Malmi-Kakkada, O.T. Valls, and C. Dasgupta, J. Low Temp. Phys. (2016) [DOI 10.1007/s10909-016-1689-3].
- [38] N.V. Prokof'ev and B.V. Svistunov. Phys. Rev. Lett. **94**, 155302 (2005).
- [39] L. Pollet, M. Boninsegni, A.B. Kuklov, N.V. Prokof'ev, B.V. Svistunov and M. Troyer. Phys. Rev. Lett. **98**, 135301 (2007).
- [40] M. Boninsegni, A.B. Kuklov, L. Pollet, N.V. Prokof'ev, B.V. Svistunov and M. Troyer, Phys. Rev. Lett. **99**, 035301 (2007).
- [41] J. Toner, Phys. Rev. Lett. **100**, 035302 (2008).
- [42] D. Goswami, K. Dasbiswas, C.-D. Yoo, and A.T. Dorsey. Phys. Rev. B **84**, 054523 (2011).
- [43] S.I. Shevchenko, Sov. J. Low Temp. Phys **14**, 553 (1988).
- [44] C. Dasgupta and O.T. Valls, Phys. Rev. B **82**, 024523 (2010).
- [45] D. Aleinikava, E. Dedits, A.B. Kuklov and D. Schmeltzer, Europhys. Lett. **89**, 46002 (2010).
- [46] D. Aleinikava, E. Dedits and A.B. Kuklov. J Low Temp Phys. **162**: 464-475 (2011).
- [47] S. Balibar, Nature **464**, 176 (2010); Physics **3**, 39 (2010).
- [48] A.N. Malmi-Kakkada, O.T. Valls, and C. Dasgupta, Phys. Rev. B **90**, 024202 (2014).
- [49] E.P. Gross. Nuovo Cimento **20** 3 (1961).
- [50] L.P. Pitaevskii. Sov. Phys. JETP **13** 2 (1961).
- [51] F. Dalfovo, S. Giorgini, L. P. Pitaevskii and S. Stringari, Rev. Mod. Phys. **71**, 463 (1999); S. Giorgini, L.P. Pitaevskii and S. Stringari, *ibid* **80**, 1215 (2008).
- [52] L.P. Pitaevskii. Sov. Phys. JETP. **35**, 282(1959).
- [53] S. Choi, S.A. Morgan, and K. Burnett. Phys. Rev. A **57**, 4057 (1998).
- [54] M. Kunimi and Y. Kato, J. Low Temp. Phys. **175**, 201 (2014).
- [55] A. Cidrim, F. E. A. dos Santos, L. Galantucci, V. S. Bagnato, and C. F. Barengghi, Phys. Rev. A **93**, 033651 (2016).
- [56] Z. Hadzibabic, P. Kruger, M. Cheneau, S.P. Rath and J. Dalibard. New Jour. of Phys. **10**, 045006 (2008).
- [57] K. Dasbiswas, D. Goswami, C.-D. Yoo and A.T. Dorsey. Phys. Rev. B **81**, 064516 (2010).
- [58] K. Kasamatsu, M. Tsubota and M. Ueda. Phys. Rev. A. **67**, 033610 (2003).
- [59] N.P. Proukakis, N.G. Parker, C.F. Barengghi, and C.S. Adams. Phys. Rev. Lett. **93**, 130408 (2004).
- [60] C.J. Pethick and H. Smith, *Bose Einstein Condensation in Dilute Gases*, Cambridge University Press, Second Edition, Cambridge, UK (2008), p.175 (for  $\xi_{SF}$ ) and p. 154 (for  $a_s$ ).
- [61] M. Boninsegni and N.V. Prokof'ev. Rev. Mod. Phys. **84**, 759 (2012).
- [62] R. A. Aziz. Inert Gases (M. L. Klein, ed.). Springer-Verlag, (1984).
- [63] W.M. Saslow. Phys. Rev. B **15**, 173 (1977); J. Low Temp. Phys. **169**, 248-263 (2012).
- [64] P. Muruganandam and S. K. Adhikari, Comput. Phys. Commun. **180**, 1888 (2009).